Combined Virtual/Experimental Multicomponent Solid Forms Screening of Sildenafil: New Salts, Cocrystals, and Hybrid Salt−Cocrystals

Rafael Barbas,[†] Mercè Font-Bardia,[§] Anant Paradkar,[‖] Christopher A. Hunter,[‡] and Rafel Prohens [*,†,⊥]

†Unitat de Polimorfisme i Calorimetria, Centres Científics i Tecnològics and §Unitat de Difracció de Raigs X, Centres Científics i Tecnològics, Universitat de Barcelona, Baldiri Reixac 10, 08028 Barcelona, Spain
‖Centre for Pharmaceutical Engineering Science, School of Pharmacy, University of Bradford, Bradford, U.K.
‡Department of Chemistry, University of Cambridge, Cambridge, U.K.
⊥Center for Intelligent Research in Crystal Engineering S.L., Palma de Mallorca, Illes Balears, Spain

43   **ABSTRACT:**

44

45   New multicomponent solid forms of sildenafil have been discovered

46   by means of a combined virtual/experimental cocrystal screening. Coformer

47   selection of candidates was conducted based on an in silico screening method from

48   a database of more than 2000 organic compounds, and the intensive experimental

49   screen produced 23 new solid forms. Since the 12 coformers chosen have a

50   combination of phenol and carboxylic acid groups, a variety of cocrystals, salts, and

51   hybrid salt-cocrystals were discovered and characterized.

52

53
54
55
56
57
58
59
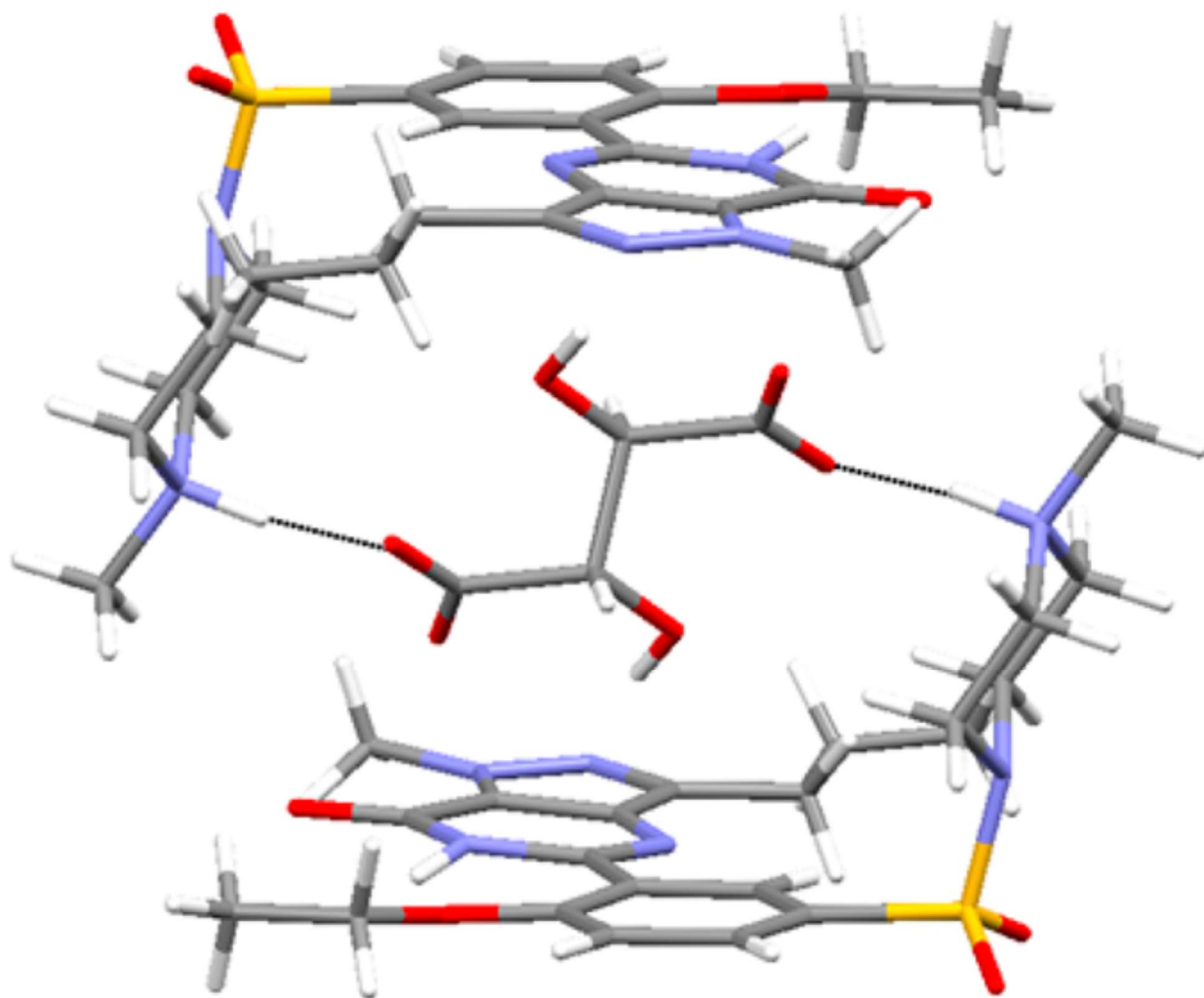
1. INTRODUCTION

Cocrystals of active pharmaceutical ingredients (APIs) have received massive attention over the past decade because they offer many opportunities to improve physicochemical properties of drugs.1,2 Indeed, solubility is one of the most important properties for a drug compound since it has a direct impact on bioavailability, and the cocrystal approach is a versatile toolbox to tune this and another important property3,4 such as stability5 because of the high number of available potential coformers. On February 2018, the Food and Drug Administration (FDA) released a final guidance titled "Regulatory Classification of Pharmaceutical Co-Crystals Guidance for Industry",6 providing applicants planning to submit new drug applications with information on the regulatory classification of pharmaceutical cocrystals, classifying them as a new form of the API, comparable in that respect to polymorphs, hydrates, salts, etc. The FDA asks the applicants to provide evidence to demonstrate that "both the API and coformers are present in the unit cell" and "the component API and coformer co-exist in the cocrystal which interact nonionically". The FDA guidance suggests that the applicant consider the difference of ΔpKa between the API and the coformer or to provide evidence that proton transfer has not occurred in the lattice by means of spectroscopic tools or other orthogonal approaches. Thus, from a regulatory point of view, it is very important to assess the proton transfer in a multicomponent Sildenafil, the active principle of Viagra, is the first oral drug used for the medical treatment of erectile dysfunction in elderly patients, and it was initially used as an antihypertensive drug8,9 but due to its poor aqueous solubility and low bioavailability it is generally formulated as sildenafil citrate.10 This solid form still exhibits moderate bioavailability, and this is the reason why some efforts have been conducted to discover new salts and cocrystals with enhanced physicochemical properties. In this sense, a sildenafil/acetylsalicylic cocrystal exhibiting enhanced intrinsic dissolution rate compared to sildenafil citrate has been reported.11 Moreover, pharmacokinetics of salts and cocrystals of sildenafil with dicarboxylic acids has been studied, and the glutarate salt was revealed to be a good candidate for alternative formulation of the citrate salt.12 The crystal structures of sildenafil base, sildenafil citrate monohydrate, sildenafil saccharinate, and sildenafil acesulfamate have been published in the literature,13,14 and some of us have described a polymorph of sildenafil free base and new solvates.15,16 With the aim to discover new multicomponent forms and extend the solid state knowledge of this important API, we have conducted a combined virtual/experimental salt/cocrystal screening by using a broad set of thermodynamic and kinetic experimental conditions. Twenty-three new solid forms of sildenafil, including salts, cocrystals, and hybrid salt−cocrystals, have been discovered and some of their crystal structures solved.

2. MATERIALS AND METHODS

2.1. Materials. Sildenafil (SIL) used in this study was of reagent grade and used as received from Polpharma (form I). The coformers quercetin (QUE), methyl gallate (MEG), tartaric acid (TAR), 3-hydroxybenzoic acid (3-HBA), 4-hydroxybenzoic acid (4-HBA), resorcinol (RES), 3,4-dihydroxybenzoic acid (3,4-DHBA), and caffeic acid (CAF) were purchased from Sigma-Aldrich.

2.2. Methods. 2.2.1. Virtual Cocrystal Screening. For each compound, the molecule was drawn in an extended conformation and energy minimized using the molecular mechanics methods implemented in TorchLite.17 Gaussian 09 was used to optimize the geometry and calculate the MEPS on the 0.002 Bohr Å−3 electron density isosurface using density functional theory (DFT) and a B3LYP/6-31G* basis set.18 The MEPS was converted into SSIPs using in-house software.19

2.2.2. Cocrystal Screening. Screening through liquid assisted grinding experiments (LAG) was conducted by grinding 20−35 mg of a 1:1 mixture of SIL and each coformer together with one drop of different solvents using a Retsch MM 2000 grinding mill. The samples were placed in 2 mL volume stainless steel jars, along with two stainless tungsten grinding balls of 3 mm diameter. Grinding was performed for 15−30 min, with a frequency of the mill of 30 Hz. Finally, the samples were collected immediately without prior drying for powder X-ray diffraction (PXRD) analysis. The formation of a new solid form was determined by comparing PXRD patterns of starting materials and products from cocrystal screening LAG experiments. Screening through reaction crystallization (RC) was conducted by preparing a saturated solution of the most soluble component (SIL or coformer) in different solvents in a sealed vial under stirring. A small quantity of the less soluble component was added until it did not dissolve anymore. The suspension was stirred at different times, and the resulting solids were filtered and analyzed by PXRD. Screening through solvent mediated transformations (SMT) were conducted by preparing suspensions of SIL and coformer in different molar ratios (40−1200mg of the final mixture) in selected solvents. The sealed vials were stirred for different times, and the resulting solids were filtered and analyzed by PXRD.

2.2.3. Solution Crystallization. Solutions of SIL/coformer in a 1:1 molar ratio (10−20 mg of the final mixture) were prepared in different solvents and heated in a heating stainless steel block. The heater was switched off, and the solutions were allowed to slowly cool down to 25°C inside the heating block. The samples which did not crystallize were tightly sealed and kept at 25 °C until precipitation was observed.

2.2.4. Synthesis of the Different Crystal Forms of Sildenafil. Details of synthesis and characterization of each form can be found in Supporting Information (see section 1 and Table S1). Stoichiometry has been assessed based on NMR and thermogravimetric analysis (TGA) measurements when the crystal structure is not available. In those cases where the crystal structure has not been solved, the definition of the form as a salt or a cocrystal has been done based on the probability of proton transfer determined with eq 3.

Twenty-three multicomponent forms of SIL (cocrystals, salts, and hybrid salt−cocrystal) have been obtained through a cocrystal screening with 8 out of the 12 coformers used. Five cocrystal forms of SIL have been obtained with three coformers: two forms with quercetin in a 1:1 stoichiometry (one as an isopronanol solvate, SILQUE I, and one as a tetrahydrofuran solvate, SIL-QUE II); two with resorcinol in two different stoichiometries (one in a 1:1 molar ratio, SIL-RES I, and one in a 1:2 molar ratio, SIL-RES II); one form with methyl gallate in a 1:1 stoichiometry, SIL-MEG. Fourteen salts of SIL have been obtained with five coformers: one form with 3,4-dihydroxybenzoic acid in a 1:1 stoichiometry as an isopropanol solvate, SIL-3,4-DHBA I; four forms with tartaric acid in two different stoichiometries: two in a 1:1 molar ratio (an anhydrous form, SIL-TAR I, and an isopropanol solvate, SIL-TAR III); two in a 2:1 molar ratio (an anhydrous form, SIL-TAR II, and an isopropanol solvate, SIL-TAR IV); two forms with caffeic acid in a 2:3 stoichiometry (one as an anhydrous form, SIL-CAF I, and one as a monohydrate, SIL-CAF II); three forms with 3-hydroxybenzoic acid in a 1:1 stoichiometry (one as an acetonitrile solvate, SIL-3-HBA I, one as a tetrahydrofuran solvate sesquihydrate, SIL-3-HBA II, and one as an anhydrous form, SIL-3-HBA III); four forms with 4-hydroxybenzoic acid in a 1:1 stoichiometry (two as anhydrous forms, SIL-4-HBA I and SIL-4-HBA III, one as a hemiisopropanol solvate, SIL-4-HBA II, and one as a tetrahydrofuran solvate, SIL-4-HBA IV). Four hybrid salt-cocrystal forms of SIL have been obtained with two coformers: three forms with 3,4-dihydroxybenzoic acid in two different stoichiometries (two of them in a 1:2 molar ratio as acetonitrile solvates, SIL-3,4-DHBA II

153 and SIL-3,4-DHBA III, and one in a 2:3 molar ratio as a dehydrate, SIL-3,4-DHBA IV) and finally one
154 form with 3-hydroxybenzoic acid in a 2:3 stoichiometry as a dehydrate, SIL-3-HBA IV.
155 2.2.5. X-ray Crystallographic Analysis. Single crystal X-ray diffraction intensity data of the different
156 crystal forms of sildenafil were collected using a D8 Venture system equipped with a multilayer
157 monochromator and a Mo microfocus ($\lambda = 0.71073$ Å). Frames were integrated with the Bruker SAINT
158 software package using a SAINT algorithm. Data were corrected for absorption effects using the
159 multiscan method (SADABS).[20] The structures were solved and refined using the Bruker SHELXTL
160 Software Package, a computer program for automatic solution of crystal structures and refined by
161 fullmatrix least-squares method with ShelXle Version 4.8.0, a Qt graphical user interface for SHELXL
162 computer program.[21]
163 Powder X-ray diffraction patterns were obtained on a PANalytical X'Pert PRO MPD diffractometer in
164 transmission configuration using Cu Kα1 + 2 radiation ($\lambda = 1.5406$ Å) with a focusing elliptic mirror
165 and a PIXcel detector working at a maximum detector's active length of 3.347°. Configuration of
166 convergent beam with a focalizing mirror and a transmission geometry with flat sample sandwiched
167 between low absorbing films measuring from 2 to 40° in 2θ, with a step size of 0.026° or from 2 to 70°
168 in 2θ, with a step size of 0.013° with measuring times of 30 min to 4 h. The powder diffractograms were
169 indexed, and the lattice parameters were refined by means of LeBail fits by means of Dicvol04,[22] and
170 the space groups were determined from the systematic absences. A summary of crystal data and relevant
171 refinement parameters are given in Tables 1 and 2.
172 2.2.6. Differential Scanning Calorimetry (DSC). Differential scanning calorimetry analysis were carried
173 out by means of a Mettler-Toledo DSC-822e calorimeter. Experimental conditions: aluminium crucibles
174 of 40 μL volume, atmosphere of dry nitrogen with a 50 mL/min flow rate, and heating rate of 10 °C/min.
175 The calorimeter was calibrated with indium of 99.99% purity (m.p.: 156.4 °C, ΔH: 28.55 J/g).
176 2.2.7. Thermogravimetric Analysis (TGA). Thermogravimetric analyses were performed on a Mettler-
177 Toledo TGA-851e thermobalance. Experimental conditions: alumina crucibles of 70 μL volume,
178 atmosphere of dry nitrogen with 50 mL/min flow rate, and a heating rate of 10 °C/min.
179 2.2.8. Nuclear Magnetic Resonance (NMR). Proton nuclear magnetic resonance (1H NMR) spectra was
180 recorded on a Varian Mercury 400 (400 MHz). Chemical shifts for proton are reported in parts per
181 million (ppm) downfield from tetramethylsilane and are referenced to residual proton in the NMR
182 solvent (DMSO-d6: δ 2.50). Experimental conditions: delay: 1; pulse: 45°; scans: 32 or 64.
183 2.2.9. Dissolution Study. The dissolution measurements were carried out only with the solid forms that
184 could be obtained pure in amounts sufficient to perform a dissolution study: pure sildenafil, salts of
185 sildenafil with citric acid, tartaric acid, 3-HBA and 3,4-DHBA, a cocrystals with RES, QUE, and two
186 hybrid salt-cocrystals of sildenafil with 3,4-DHBA. The dissolution was determined in 0.1 N HCl (pH
187 1.2), phosphate buffer pH 6.5, and a biorelevant dissolution medium fasted state simulated intestinal
188 fluid (FaSSIF) at 25 °C. For dissolution studies 40 mg of crystalline compounds were added to the
189 dissolution medium stirred at 100 rpm over 24 h, and samples were withdrawn at 1 and 24 h. The
190 amount of SIL dissolved in 1 h (D1h) and 24 h (D24h) was determined using the HPLC technique. The
191 details about dissolution medium and HPLC method are provided in Supporting Informatiom.
192
193
194

3. RESULTS AND DISCUSSION

3.1. Virtual Cocrystal Screen. We selected the coformers for experimental screening based on the virtual cocrystal screening methodology developed by some of us to predict the probability of cocrystal formation.[23] This computational tool has been validated using experimental data extracted from the literature.

The difference between the calculated energy of the cocrystal and the pure components was used to rank potential cofomers.[24] This approach uses surface site interaction points (SSIPs) calculated from the ab initio molecular electrostatic potential surface (MEPS) of the isolated molecule in the gas phase.[19,25] The interaction of a molecule with its environment is described by a discrete set of SSIPs, each represented by an interaction parameter, ε_i, which is positive for a H-bond donor site (or positive region on the MEPS) and negative for a H-bond acceptor site (or negative region on the MEPS). The energy of interaction between two SSIPs, i and j, is given by the product $\varepsilon_i\varepsilon_j$. We assume that pairwise interactions between SSIPs are optimized in a solid, and this provides a method for evaluating the interaction site pairing energy of a solid without knowledge of the crystal structure.[26] The most positive SSIP is paired with the most negative SSIP, the next most positive SSIP with the next most negative, and so on, giving a hierarchical list of interactions.[27,28] This interaction site pairing strategy provides a straightforward method for estimating the energy of a solid, E (eq 1). The same approach can be used to estimate the energy of a cocrystal, and the difference between the interaction site pairing energies of the cocrystal and the pure components, ΔE, can be used to estimate the probability of cocrystal formation (eq 2).

$$E = \Sigma\varepsilon_i\varepsilon_j \tag{1}$$

$$\Delta E = -(E_{cc} - E_1 - E_2) \tag{2}$$

where E_1, E_2, and E_{cc} are the interaction site pairing energies of the pure solids, 1 and 2, and a 1:1 cocrystal respectively. Note that this definition means that ΔE is always positive, and a large value indicates a high probability of cocrystal formation.

Some of us have previously applied the method to successfully predict the formation of new cocrystals,[29,30] and in this work we have followed this theoretical approach to guide the selection of a limited number of coformers to test experimentally. Thus, the difference between the interaction site pairing energies of the 1:1 cocrystal and the pure components was calculated for each sildenafil/coformer combination using a coformer database which contains more than 2000 organic compounds (including 860 products from the GRAS list). The coformers were ranked in order of decreasing ΔE, and only 12 coformers were chosen from the top 100 compounds according to toxicity criteria and probability of success in a cocrystallization experiment (Table 3). This theoretical approach

231 defines an energy threshold of 11kJ/mol where the probability of cocrystal formation is higher than

232 50%. Thus, only coformers with ΔE > 11 kJ/mol were chosen for experimental screening

233 Since sildenafil has a strong basic group, the formation of salts with strong carboxylic acids is expected.

234 In fact, the formation of a salt or a cocrystal can be assessed based on the "rule of thumb"[31] which

235 states that salts are formed when ΔpKa [pKa(base) − pKa(acid)] ≥ 3, and a cocrystal is expected when

236 this value is ≤0, the combinations with a value 0 ≤ [pKa(base) − pKa(acid)] ≤ 3 being much less reliable

237 and falling around a "salt-cocrystal continuum" region.[32] This uncertainty motivated the analysis and

238 correlation by Cruz-Cabeza[33] of a big set of experimental cocrystal/salt data in order to develop a more

239 reliable equation to predict the salt/cocrystal outcome. According to this statistical analysis, eq 3 allows

240 prediction of the probability of proton transfer around the region of ΔpKa values between −1 and 4.

241

242 $P(\%) = 17\Delta pKa + 28$ (3)

243

244 Sildenafil has a basic functional group (piperazine) with a pKa value of 6.78,[34] and we have applied this

245 statistical approach to the coformers with acidic groups selected from the virtual cocrystal screening to

246 assess the probability of salt formation (Table 4). Coformers with acidic groups such as

247 (3hydroxybenzoic acid, 4-hydroxybenzoic acid, caffeic acid, 3,4-dihydroxybenzoic acid, and tartaric

248 acid) were expected to form salts. However, salt stoichiometry is an important outcome not always easy

249 to predict because hybrid salt−cocrystal forms are also possible. In this sense, there are interesting

250 examples in the literature with unexpected stoichiometries due to the presence of nonionized molecules

251 in the crystal structure such as the p-coumaric acid/quinine[39] or the trans-N,N′-

252 dibenzyldiaminocyclohexane/2,3-dichlorophenylacetic acid[40] hybrid salt−cocrystals. Moreover,

253 Aakeröy et al.[41] suggested in a structural analysis of more than 80 cocrystals and salts formed between

254 carboxylic acids and Nheterocycles that the formation of unexpected hybrid salt−cocrystals could be

255 because carboxylate moieties are not readily satisfied by a single hydrogen-bond donor making

256 necessary the presence of neutral carboxylic acids in the crystal structure. We have examined the

257 Cambridge Structural Database (version 5.39, 2018) in order to assess the formation of hybrid

258 salt−cocrystal forms in multicomponent crystals containing a piperazine ring (the basic group of

259 sildenafil) and a carboxylic acid (Figure 3).

260 A total of 247 crystal structures containing atomic coordinates were found and classified as salt,

261 cocrystal, or hybrid salt−cocrystal according to the C−O bond lengths of the carboxylate moiety.

262 Although 184 structures showed total proton transfer between donor and acceptor, 63 of them revealed

263 that cocrystals or mixed salt-cocrystals were formed. This encouraged us to test the carboxylic acids

264 previously chosen in the virtual cocrystal prediction. Table 5 summarizes the results of this structural

265 analysis.

266 **3.2. Salt/Cocrystal Screening.** With the aim to discover new salts or cocrystals of sildenafil ,an

267 extensive multicomponent solid forms screening was conducted by using a broad set of thermodynamic

268 and kinetic experimental conditions from a variety of 54 solvents,42 which produced 194 individual

269 crystalline solids (see Supporting Information for experimental and characterization details).

270 **3.3. Crystal Structures Analysis**. The crystal structures of 5 out of the new 23 forms of sildenafil have

271 been solved by single crystal X-ray diffraction, and the following analysis shows that in all cases salts or

272 hybrid salt-cocrystals have been formed with tartaric acid, 3-hydroxybenzoic acid, and 3,4-

273 dihydroxibenzoic acid.

274 3.3.1. Tartaric Acid Salt Isopropanol Hemisolvate (SIL-TAR IV). Tartaric acid salt isopropanol

275 hemisolvate crystallizes with one molecule of sildenafil cation, half molecule of tartrate dianion, and

276 half disordered molecule of isopropanol in the asymmetric unit. Transfer of both protons of tartaric acid

277 has been deduced since tartrate C−O distances are 1.183(9) and 1.232(8) Å. The dianion, which shows

278 disorder between two conformations (in a 1:1 ratio), is encapsulated between two molecules of sildenafil

279 establishing strong charge-assisted hydrogen bonds. Sildenafil/tartrate cages are packed with a

280 combination of electrostatic interactions between sulphonamide moieties in a self-association fashion

281 and weak hydrogen bonds between N-methylpyrazole rings (Figures 4 and 5). Molecular cavities are

282 present and occupied by disordered molecules of isopropanol.

283 3.3.2. Hybrid 3-Hydroxybenzoic Acid Salt−Cocrystal Monohydrate (SIL-3-HBA IV). The hybrid

284 salt−cocrystal formed by 3-hydroxybenzoic acid and sildenafil crystallizes with one molecule of

285 sildenafil cation, one molecule of the carboxylate, half molecule of the carboxylic acid, and one

286 molecule of water in the asymmetric unit. Chains of selfassembled sildenafil cations are formed through

287 strong hydrogen bonds between the piperazinium ring and the carbonylic oxygen. As expected, strong

288 charge-assisted hydrogen bonds are formed between the carboxylate anion and the piperazinium cation,

289 but one molecule of the nonionized carboxylic acid interacts with the carboxylate anion via the phenol

290 and carboxylic hydrogen in an alternate manner (Figure 9). Weak antiparallel dipole−dipole interactions

291 between stacked pyrimidinone rings are established conferring extra stabilization to the crystal (Figure

292 8).

293 In addition, one molecule of water is also present acting as a bridge between carboxylates (Figure 6).

294 Nonionized 3-hydroxybenzoic acid molecules are located in channels establishing strong hydrogen

295 bonds with other 3-hydroxybenzoate molecules (Figure 7).

296 3.3.3. 3-Hydroxybenzoic Acid Salt THF Hemisolvate Sesquihydrate (SIL-3-HBA II). The salt formed

297 by 3-hydroxybenzoic acid and sildenafil crystallizes with one molecule of sildenafil cation, one

298 molecule of the carboxylate, half disordered molecule of THF, and 1.5 molecules of water in the

299 asymmetric unit. In spite of the different degree of proton transfer, this solid form is isostructural to the

300 hybrid 3-hydroxybenzoic acid saltcocrystal, and the same interactions between sildenafil and 3-

301 hydroxybenzoate molecules are established. Moreover, identical channels are formed but filled by

302 disordered tetrahydrofuran and water molecules instead of molecules of 3-hydroxybenzoic acid. Only

303 small differences between both structures are present like, for instance, centroid−centroid distances

304 measured betwee pyrimidinone rings and torsion angles of propyl groups (Figure 8).

305 3.3.4. Hybrid 3,4-Dihydroxybenzoic Acid Salt−Cocrystal Monohydrate (SIL-3,4-DHBA IV). The
306 hybrid salt-cocrystal formed by 3,4-dihydroxybenzoic acid and sildenafil crystallizes with one molecule
307 of sildenafil cations, one molecule of the carboxylate, half molecule of the carboxylic acid, and one
308 molecule of water in the asymmetric unit. This solid form is isostructural to the hybrid 3-
309 hydroxybenzoic acid salt−cocrystal. The presence of an extra phenol group in the 3,4-dihydroxybenzoic
310 acid only reinforces the same packing without disrupting any of the main observed interactions in the
311 hybrid 3-hydroxybenzoic acid salt−cocrystal. Figure 9 shows chains of carboxylate molecules linked by
312 water molecules in both structures.

313 3.3.5. Hybrid 3,4-Dihydroxybenzoic Acid Salt−Cocrystal Acetonitrile Disolvate (SIL-3,4-DHBA II).
314 The hybrid 3,4-dihydroxybenzoic acid salt−cocrystal acetonitrile disolvate crystallizes with one
315 molecule of the sildenafil cation, one molecule of the carboxylate, one molecule of the carboxylic acid,
316 and two molecules of acetonitrile in the asymmetric unit. In a similar way that the tartaric acid salt,
317 instead of catemeric chains of sildenafil cations, self-assembled dimers are formed through charge-
318 assisted hydrogen bonds (Figure 10).

319 However, the antiparallel dipole−dipole interactions between stacked pyrimidinone rings are not
320 observed in this form. This is the only structure of this family of hybrid salts−cocrystals where water is
321 not present, and this produces a different architecture of the coformer self-assembling, which consists of
322 layers of alternate carboxylic/carboxylate interactions (Figure 11).

323 **3.4. Dissolution Study.** The dissolution studies were carried out at pH 1.2, pH 6.5, and FaSSIF (pH
324 6.5), which represent the average pH values of the fast state stomach and intestine, respectively. SIL has
325 pH dependent solubility which decreases with an increase in pH. One of the major challenges in the
326 dissolution study of multicomponent entities is continuous change in the solution composition due to
327 precipitation of either of the component over the dissolution testing period. The solubility data generated
328 may be erroneous due to limitations of the analytical method; for example, estimations carried out by
329 UV spectrophotometry are subject to the overlap in the absorption spectra of the two components. We
330 have used the HPLC method to quantify the amount of SIL dissolved; hence we see some difference in
331 reported dissolutions compared to the previous SIL salt dissolution data reported.[43] Figures 12, 13, and
332 14 (and Figures S75−S77 of the Supporting Information) show the dissolution data.

333 At pH 1.2 the amount dissolved from SIL salts was significantly higher than the cocrystals and the
334 hybrid salt−cocrystal forms. The hybrid salt−cocrystals showed poor dissolution performance compared
335 to cocrystals. The D1h and D24h values for SIL-TAR I were higher than for SIL-CIT, a commercially
336 used salt of SIL. At pH 1.2 in the salt category SILTAR > SIL-3-HBA I > SIL-CIT > SIL-3,4-DHBA I.
337 On the other hand D1h for SIL-RES II > SIL-QUE I and SIL-QUE II. As expected, the amount
338 dissolved at pH 6.5 was at least 10 times lower than the amount dissolved at pH 1.2. But in both
339 conditions, the amount of SIL dissolved was significantly higher for salts than for cocrystals and hybrid
340 salt−cocrystals. Most of the cocrystals and hybrid salt−cocrystals did not provide any release of SIL at
341 pH 6.5 or even in FaSSIF, which contains an additive like lecithin included in the dissolution media.

342   Thus, although an exhaustive solubility study of the new forms was not the main objective of this

343   research, our data suggest that SILTAR could be a potential alternative (in terms of bioavailability) to

344   the commercial citrate salt of sildenafil.

345

346

347

348

349

350 **4. CONCLUSION**

351

352 In summary, we have revisited the multicomponent solid form landscape of sildenafil by conducting a

353 combined virtual and experimental screening. Twenty-three new solid forms have been discovered and

354 characterized, and dissolution data have been measured for some of the solid forms suggesting the new

355 tartrate salt as a potential alternative to the marketed citrate salt. The analysis of the five crystal

356 structures solved by SXRD showed a variety of salts and hybrid salt−cocrystals with different hydrogen

357 bond architectures and presence of solvent channels. This study extends the knowledge about the solid

358 state of this important drug compound, contributes with new cases to the body of data of unexpected

359 stoichiometric hybrid salt−cocrystals, and it is a new example of successful application of combined

360 virtual/experimental methodologies for the discovery of new solid forms.

361

362

AUTHOR INFORMATION

Corresponding Author

*E-mail: rafel@ccit.ub.edu.

ORCID

Rafael Barbas: 0000-0002-1603-3689

Anant Paradkar: 0000-0003-1704-9858

Christopher A. Hunter: 0000-0002-5182-1859

Rafel Prohens: 0000-0003-0294-1720

Notes

The authors declare no competing financial interest.

377 **REFERENCES**

378

379 (1) Blagden, N.; de Matas, M.; Gavan, P. T.; York, P. Crystal engineering of active pharmaceutical
380 ingredients to improve solubility and dissolution rates. Adv. Drug Delivery Rev. 2007, 59,
381 617−630.

382 (2) Almarsson, O.; Zaworotko, M. J. Crystal engineering of the composition of pharmaceutical
383 phases. Do pharmaceutical co-crystals represent a new path to improved medicines? Chem.
384 Commun. 2004, 1889−1896.

385 (3) Bolla, G.; Sanphui, P.; Nangia, A. Solubility Advantage of Tenoxicam Phenolic Cocrystals
386 Compared to Salts. Cryst. Growth Des. 2013, 13, 1988−2003.

387 (4) Good, D. J.; Rodríguez-Hornedo, N. Solubility Advantage of Pharmaceutical Cocrystals. Cryst.
388 Growth Des. 2009, 9, 2252−2264.

389 (5) Liu, X.; Lu, M.; Guo, Z.; Huang, L.; Feng, X.; Wu, C. Improving the Chemical Stability of
390 Amorphous Solid Dispersion with Cocrystal Technique by Hot Melt Extrusion. Pharm. Res.
391 2012, 29, 806−817.

392 (6) Food and Drug Administration. Regulatory Classification of Pharmaceutical Co-Crystals G
393 uidance for Industry, 2018.

394 (7) Thipparaboina, R.; Kumar, D.; Mittapalli, S.; Balasubramanian, S.; Nangia, A.; Shastri, N. R.
395 Ionic, Neutral, and Hybrid Acid-Base   Crystalline Adducts of Lamotrigine with Improved
396 Pharmaceutical Performance. Cryst. Growth Des. 2015, 15, 5816−5826.

397 (8) Barnett, C. F.; Machado, R. F. Sildenafil in the treatment of pulmonary hypertension. Vasc
398 Health Risk Manag. 2006, 2, 411−422.

399 (9) Galiè, N.; Hoeper, M. M.; Humbert, M.; Torbicki, A.; Vachiery, J. L.; Barbera, J. A.; Beghetti,
400 M.; Corris, P.; Gaine, S.; Gibbs, J. S.; Gomez-Sanchez, M. A.; Jondeau, G.; Klepetko, W.;
401 Opitz, C.; Peacock, A.; Rubin, L.; Zellweger, M.; Simonneau, G. ESC Committee for Practice
402 Guidelines (CPG) Guidelines for the diagnosis and treatment of pulmonary hypertension: The
403 Task Force for the Diagnosis and Treatment of Pulmonary Hypertension of the European
404 Society of Cardiology (ESC) and the European Respiratory Society (ERS), endorsed by the
405 International Society of Heart and Lung Transplantation (ISHLT). Eur. Heart J. 2009, 30,
406 2493−2537.

407 (10) Jung, S. Y.; Seo, Y. G.; Kim, G. K.; Woo, J. S.; Yong, C. S.; Choi, H. G. Comparison of the
408   solubility and pharmacokinetics of sildenafil   salts. Arch. Pharmacal Res. 2011, 34, 451−454.

409 (11) Žegarac, M.; Lekšić, E.; Šket, P.; Plavec, J.; Bogdanović, M. D.; Bučar, D. K.; Dumić, M.;
410   Meštrović, E. A sildenafil cocrystal based on acetylsalicylic acid exhibits an enhanced intrinsic
411   dissolution rate. CrystEngComm 2014, 16, 32−35.

412 (12) Sanphui, P.; Tothadi, S.; Ganguly, S.; Desiraju, G. R. Salt and Cocrystals of Sildenafil with
413   Dicarboxylic Acids: Solubility and Pharmacokinetic Advantage of the Glutarate Salt. Mol.
414   Pharmaceutics 2013, 10, 4687−4697.

415 (13) Stepanovs, D.; Mishnev, A. Molecular and Crystal Structure of Sildenafil Base. Z. Naturforsch.,
416   B: J. Chem. Sci. 2012, 67, 491−494 CSD code QEGTUT. .

417 (14) Wang, C.; Perumalla, S. R.; Sun, C. C. Anion Exchange Reaction for Preparing Acesulfame
418   Solid Forms. Cryst. Growth Des. 2018, 18, 4215−4219.

419 (15) Barbas, R.; Font-Bardia, M.; Prohens, R. Polymorphism of Sildenafil: A New Metastable
420   Desolvate. Cryst. Growth Des. 2018, 18, 3740−3746.

421 (16) Barbas, R.; Prohens, R.; Font-Bardia, M.; Bauzá, A.; Frontera, A. Hydrogen bonding versus π-
422   interactions: their key competition in sildenafil solvates. CrystEngComm 2018, 20, 4526−4530.

423 (17) Cresset torchV10lite. http://www.cresset-group.com/products/ torch/torchlite/.

424 (18) Frisch, M. J.; Trucks, G. W.; Schlegel, H. B.; Scuseria, G. E.; Robb, M. A.; Cheeseman, J. R.;
425   Scalmani, G.; Barone, V.; Mennucci, B.; Petersson, G. A.; Nakatsuji, H.; Caricato, M.; Li, X.;
426   Hratchian, H. P.; Izmaylov, A. F.; Bloino, J.; Zheng, G.; Sonnenberg, J. L.; Hada, M.; Ehara,
427   M.; Toyota, K.; Fukuda, R.; Hasegawa, J.; Ishida, M.; Nakajima, T.; Honda, Y.; Kitao, O.;
428   Nakai, H.; Vreven, T.; Montgomery, J. A., Jr.; Peralta, J. E.; Ogliaro, F.; Bearpark, M.; Heyd, J.
429   J.; Brothers, E.; Kudin, K. N.; Staroverov, V. N.; Kobayashi, R.; Normand, J.; Raghavachari, K.;
430   Rendell, A.; Burant, J. C.; Iyengar, S. S.; Tomasi, J.; Cossi, M.; Rega, N.; Millam, J. M.; Klene,
431   M.; Knox, J. E.; Cross, J. B.; Bakken, V.; Adamo, C.; Jaramillo, J.; Gomperts, R.; Stratmann, R.
432   E.; Yazyev, O.; Austin, A. J.; Cammi, R.; Pomelli, C.; Ochterski, J. W.; Martin, R. L.;
433   Morokuma, K.; Zakrzewski, V. G.; Voth, G. A.; Salvador, P.; Dannenberg, J. J.; Dapprich, S.;
434   Daniels, A. D.; Farkas, O.; Foresman, J. B.; Ortiz, J. V.; Cioslowski, J.; Fox, D. J. Gaussian 09;
435   Gaussian, Inc.: Wallingford, CT, 2009.

436   (19)   Calero, C. S.; Farwer, J.; Gardiner, E. J.; Hunter, C. A.; Mackey, M.; Scuderi, S.; Thompson, S.;
437   Vinter, J. G. Footprinting molecular electrostatic potential surfaces for calculation of solvation
438   energies. Phys. Chem. Chem. Phys. 2013, 15, 18262−18273.

439   (20)   SADABS Bruker AXS; Madison, Wisconsin, USA, 2004; SAINT, Software Users Guide,
440   Version 6.0; Bruker Analytical X-ray Systems: Madison, WI, 1999. Sheldrick, G. M. SADABS
441   v2.03; Area-Detector Absorption Correction; University of Göttingen: Germany, 1999. Saint,
442   Version 7.60A; Bruker AXS 2008; SADABS, V. 2008-1, 2008.

443   (21)   Sheldrick, G. M. A short history of SHELX. Acta Crystallogr., Sect. A: Found. Crystallogr.
444   2008, 64, 112−122.

445   (22)   Boultif, A.; Louër, D. Indexing of powder diffraction patterns for low-symmetry lattices by the
446   successive dichotomy method. J. Appl. Crystallogr. 1991, 24, 987−993.

447   (23)   Musumeci, D.; Hunter, C. A.; Prohens, R.; Scuderi, S.; McCabe, J. F. Virtual cocrystal
448   screening. Chem. Sci. 2011, 2, 883−890.

449   (24)   Grecu, T.; Hunter, C. A.; McCabe, J.; Gardiner, E. J.; McCabe, J. F. Validation of a
450   Computational Cocrystal Prediction Tool: Comparison of Virtual and Experimental Cocrystal
451   Screening Results. Cryst. Growth Des. 2014, 14, 165−171.

452   (25)   Hunter, C. A. A surface site interaction model for the properties of liquids at equilibrium. Chem.
453   Sci. 2013, 4, 1687−1700.

454   (26)   Hunter, C. A. Quantifying Intermolecular Interactions: Guidelines for the Molecular
455   Recognition Toolbox. Angew. Chem., Int. Ed. 2004, 43, 5310−5324.

456   (27)   Etter, M. C. Hydrogen Bonds as Design Elements in Organic Chemistry. J. Phys. Chem. 1991,
457   95, 4601−4610.

458   (28)   Aakeroy, C. B.; Desper, J.; Smith, M. M. Constructing, deconstructing, and reconstructing
459   ternary supermolecules. Chem. Commun. 2007, 3936−3938.

460   (29)   Grecu, T.; Prohens, R.; McCabe, J. F.; Carrington, E. J.; Wright, J. S.; Brammer, L.; Hunter, C.
461   A. Cocrystals of spironolactone and griseofulvin based on an in silico screening method.
462   CrystEngComm 2017, 19, 3592−3599.

463   (30)   Grecu, T.; Adams, H.; Hunter, C. A.; McCabe, J. F.; Portell, A.; Prohens, R. Virtual Screening
464   Identifies New Cocrystals of Nalidixic Acid. Cryst. Growth Des. 2014, 14, 1749−1755.

465 (31) International Union of Pure and Applied Chemistry (IUPAC); Stahl, P. H.; Wermuth, C. G.,
466   Eds.; Handbook of Pharmaceutical Salts: Properties, Selection, and Use; Wiley-VCH: New
467   York, 2002.

468 (32) Childs, S. L.; Stahly, G. P.; Park, A. The Salt-Cocrystal Continuum: The Influence of Crystal
469   Structure on Ionization State. Mol. Pharmaceutics 2007, 4, 323−338.

470 (33) Cruz-Cabeza, A. J. Acid−base crystalline complexes and the pKa rule. CrystEngComm 2012,
471   14, 6362−6365.

472 (34) Gobry, V.; Bouchard, G.; Carrupt, P. A.; Testa, B.; Girault, H. H. Physicochemical
473   Characterization of Sildenafil: Ionization, Lipophilicity Behavior, and Ionic-Partition Diagram
474   Studied by Two-Phase Titration and Electrochemistry. Helv. Chim. Acta 2000, 83, 1465−1474.

475 (35) pKa value: Musialik, M.; Kuzmicz, R.; Pawłowski, T. S.; Litwinienko, G. Acidity of Hydroxyl
476   Groups: An Overlooked Influence on Antiradical Properties of Flavonoids. J. Org. Chem. 2009,
477   74, 2699−2709.

478 (36) pKa values: FooDB Database. http://foodb.ca/.

479 (37) pKa values: Internet Bond-energy Databank (iBonD). http://ibond.chem.tsinghua.edu.cn.

480 (38) pKa values: Tao, L.; Han, J.; Tao, F. M. Correlations and Predictions of Carboxylic Acid pKa
481   Values Using Intermolecular Structure and Properties of Hydrogen-Bonded Complexes. J. Phys.
482   Chem. A 2008, 112, 775−782.

483 (39) Jacobs, A.; Amombo Noa, F. M. Hybrid Salt-Cocrystal Solvate: p-Coumaric Acid and Quinine
484   System. J. Chem. Crystallogr. 2014, 44, 57−62.

485 (40) Mahieux, J.; Gonella, S.; Sanselme, M.; Coquerel, G. Crystal structure of a hybrid salt−cocrystal
486   and its resolution by preferential crystallization: ((±)trans-N,N′-
487   dibenzyldiaminocyclohexane)(2,3-dichlorophenylacetic acid)4. CrystEngComm 2012, 14,
488   103−111.

489 (41) Aakeröy, C. B.; Fasulo, M. E.; Desper, J. Cocrystal or Salt: Does It Really Matter? Mol.
490   Pharmaceutics 2007, 4, 317−322.

491 (42) Methanol, ethanol, IPA, butanol, 1-propanediol, glycerol, ethylene glycol, 2-methoxyethanol,
492   1-propanol, 1-pentanol, 1-octanol, 2,2,2-trifluoroethanol, benzyl alcohol, ACN, propionitrile,
493   MEK, acetone, MiBK, water, DMF, DMSO, pentane, heptane, cyclohexane, hexane,
494   methylcyclohexane, toluene, xylene, mesitylene, anisole, 2-nitrotoluene, nitrobenzene, AcOEt,

495   isopropyl acetate, diethylether, THF, 1-methyl-2-pyrrolidone, dimethyl ethylene glycol,

496   diisopropyl ether, dioxane, iodomethane, dichloromethane, 1,2-dichlorothane, chloroform, 1,1,1-

497   trichloroethane, 1,1,2-trichloroethane, formic acid, acetic acid, trifluoroacetic acid, propanoic

498   acid, NH3 (32%) in water, diethylamine, trimethylamine and pyridine.

499   (43)   Sanphui, P.; Tothadi, S.; Ganguly, S.; Desiraju, G. R. Salt and Cocrystals of Sildenafil with

500   Dicarboxylic Acids: Solubility and Pharmacokinetic Advantage of the Glutarate Salt. Mol.

501   Pharmaceutics 2013, 10, 4687−4697.

502

Legends to figures

Figure. 1. Molecular structure of sildenafil.

Figure. 2 SSIPs calculated for sildenafil. Blue spheres correspond to Hbond donors and red spheres to H-bond acceptors.

Figure. 3 Fragments searched in multicomponent crystals in the CSD.

Figure. 4 Crystal structure of tartaric acid salt of sildenafil. The most relevant interactions are highlighted. Channels filled by solvent molecules are highlighted with gray circles.

Figure. 5 Sildenafil/tartrate cage in the crystal structure of tartaric acid salt of sildenafil.

Figure. 6 Chains of carboxylate/carboxylic acid molecules linked by molecules of water in the hybrid 3-hydroxybenzoic salt−cocrystal monohydrate.

Figure. 7 Representation of the crystal structures of 3-hydroxybenzoic acid salt and hybrid salt−cocrystal of sildenafil. The most relevant interactions have been highlighted, and hydrogens have been partially omitted for clarity. Channels filled by THF and water molecules in the salt or 3-hydroxybenzoic molecules in the hybrid salt−cocrystal are highlighted with gray circles.

Figure. 8 Antiparallel dipole−dipole interactions established between stacked pyrimidinone rings in the crystal structures of 3-hydroxybenzoic acid salt (right) and hybrid salt-cocrystal (left). Differences in centroid−centroid distances measured between pyrimidinone rings and torsion angles of propyl groups are shown for each structure.

Figure. 9 Chains of carboxylate molecules linked by molecules of water in the hybrid 3-hydroxybenzoic acid salt−cocrystal (left) and in the hybrid 3,4-dihydroxybenzoic acid salt−cocrystal (right).

Figure. 10 Crystal structure of 3,4-dihydroxybenzoic acid hybrid salt−cocrystal. Self-assembled dimers formed through charge-assisted hydrogen bonds are highlighted. Hydrogens have been partially omitted for clarity.

Figure. 11 Layers of alternate carboxylic (blue)/carboxylate (red) interactions.

539   **Figure. 12** Comparative solubility of SIL salts, cocrystals, and hybrid salt−cocrystals in 0. 1 N HCl (pH

540   1.2).

541

542

543   **Figure. 13** Comparative solubility of SIL salts, cocrystals, and hybrid salt−cocrystals in phosphate

544   buffer pH 6.5.

545

546

547   **Figure. 14** Comparative solubility of SIL salts, cocrystals, and hybrid salt−cocrystals in FaSSIF.

548

549

550

551
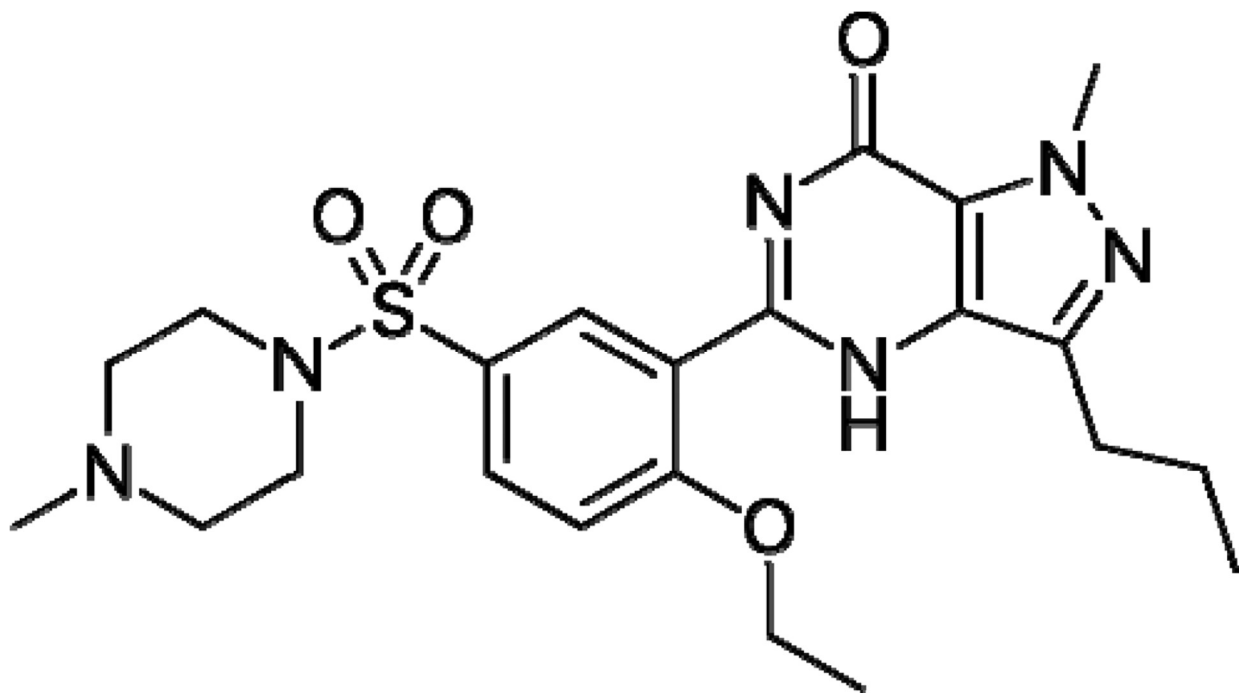
FIGURE 1

552

553

554

555
556
557

558   **FIGURE 2**

559

560

561

562

FIGURE 3

563

564

565

566

567
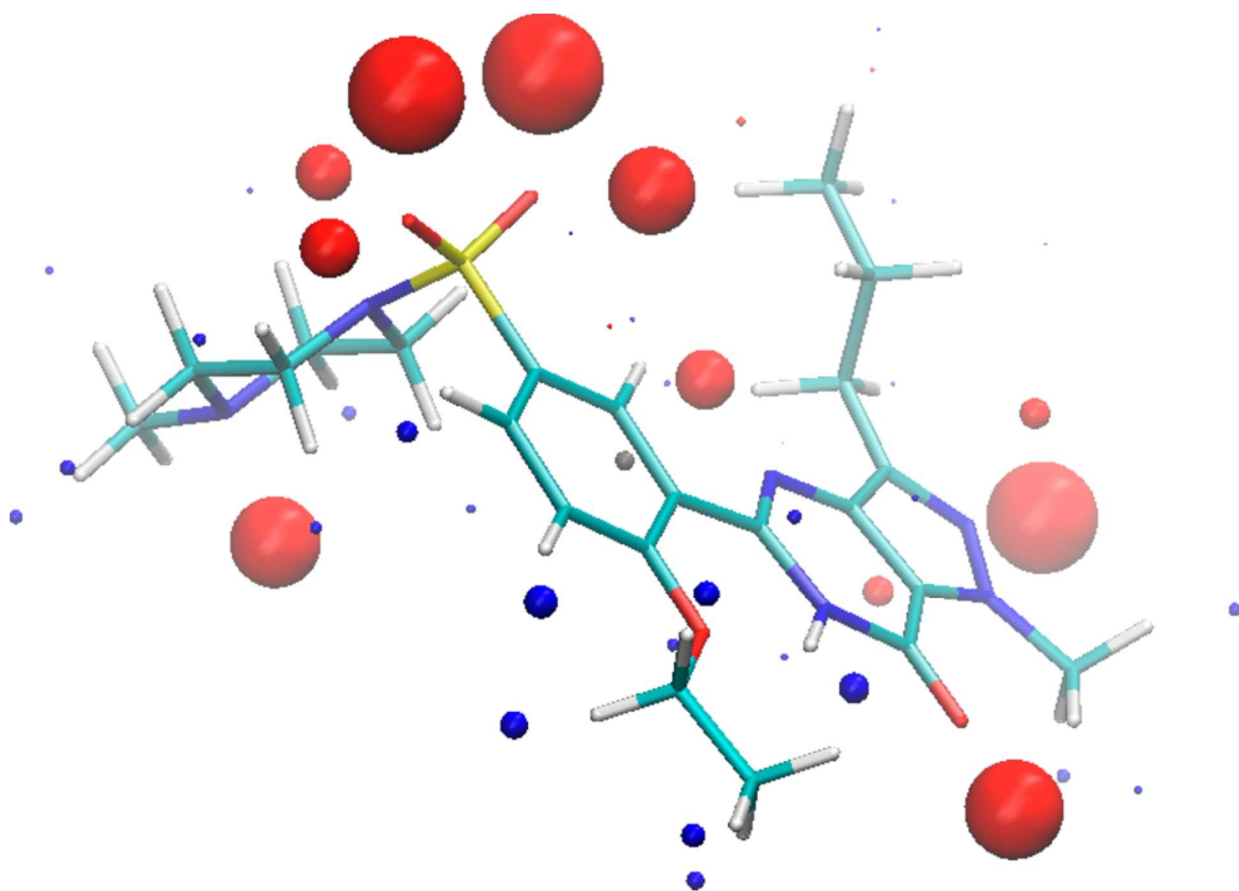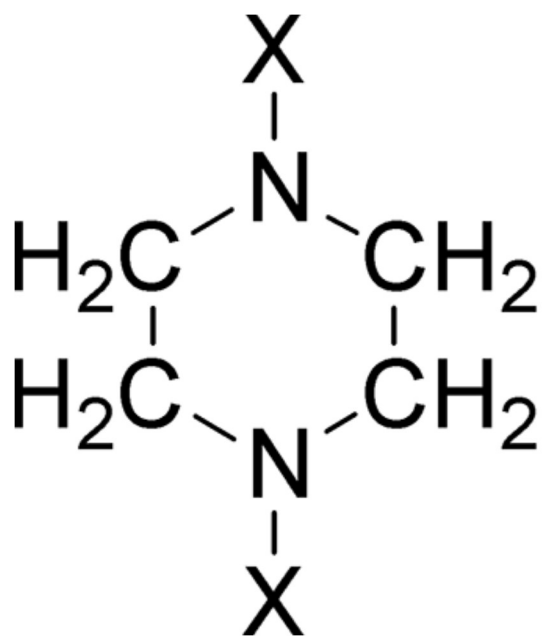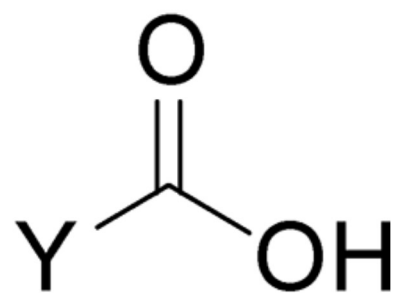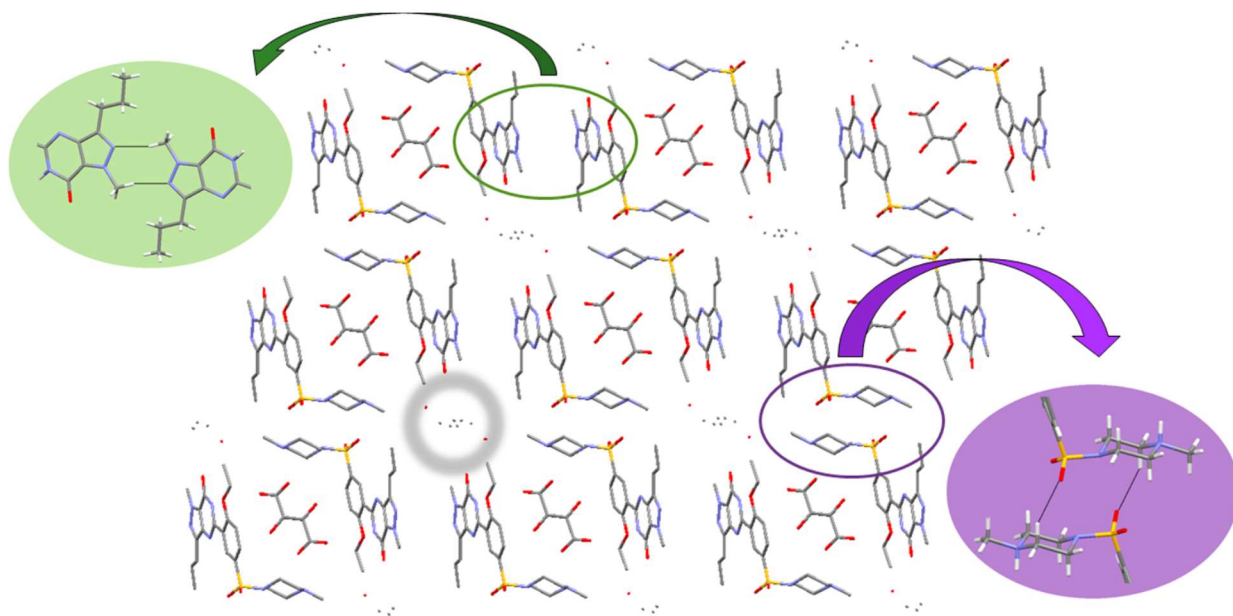
FIGURE 4

573 **FIGURE 5.**

574

575

576

577

578
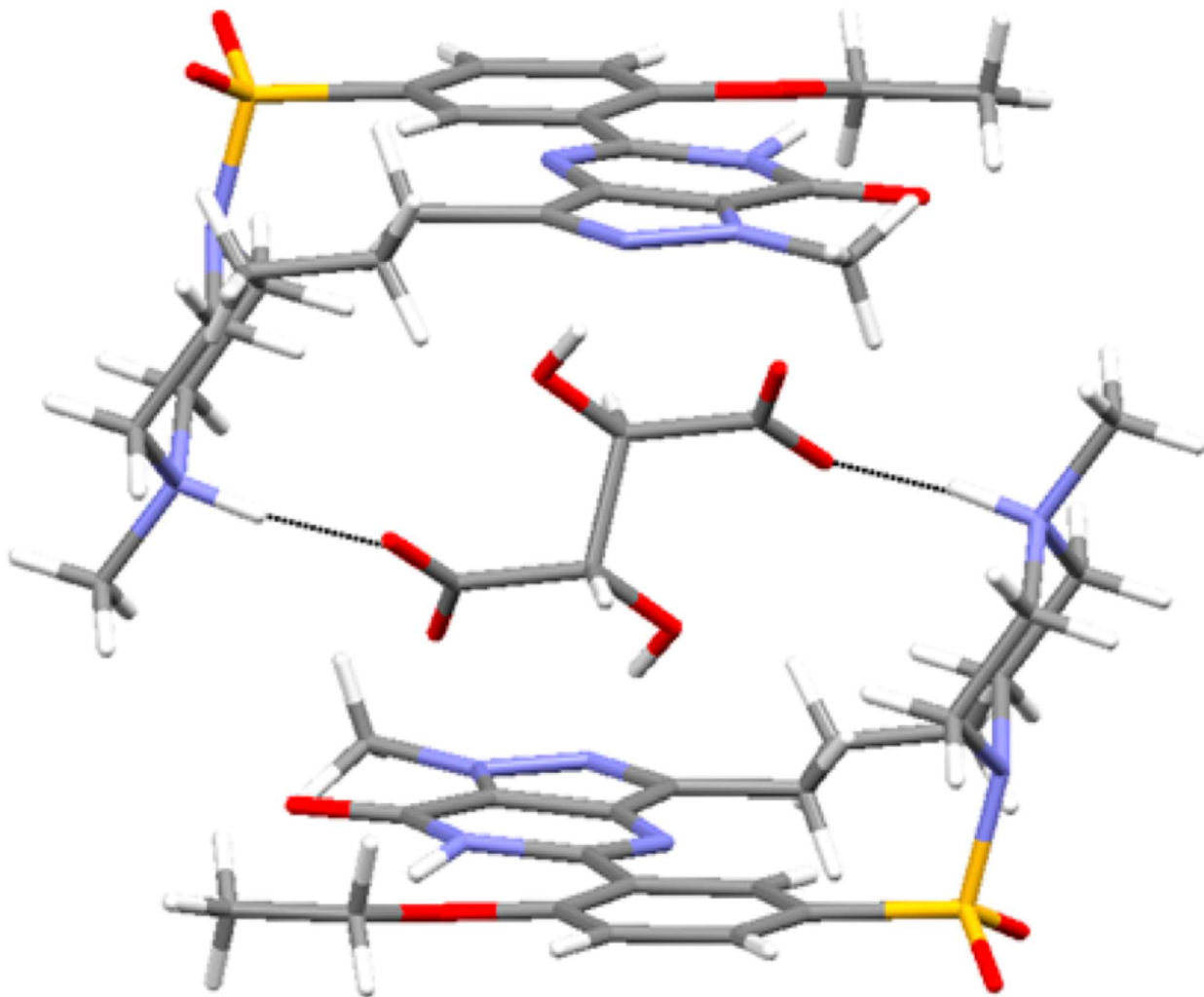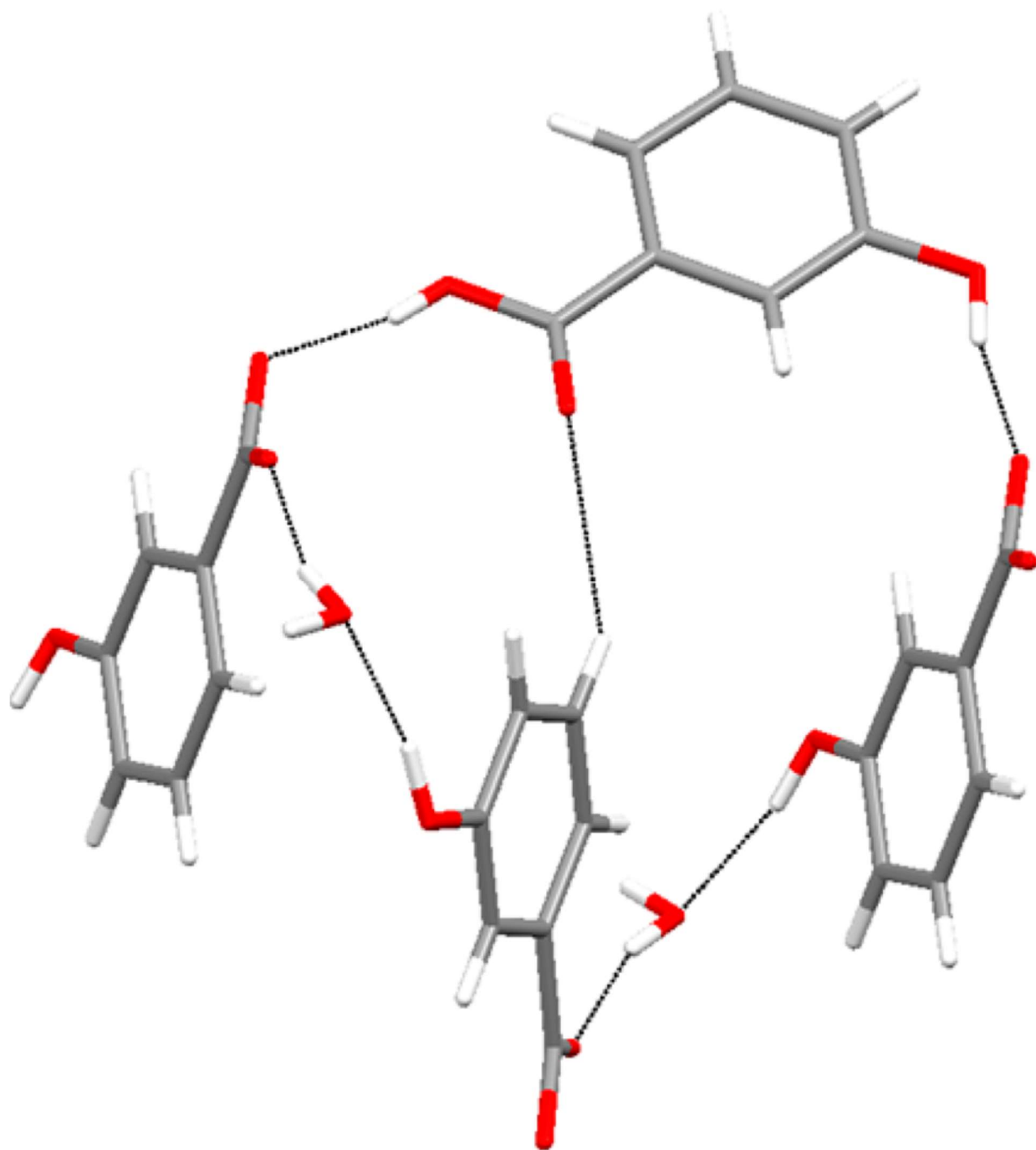
FIGURE 6.

584 **FIGURE 7.**

585

586

587

588

589

590

591

FIGURE 8.

$d_{centroid}$

3.45 Å   3.54 Å

Torsion angle

Hybrid   θ: 6 °   θ: 180 °   Salt
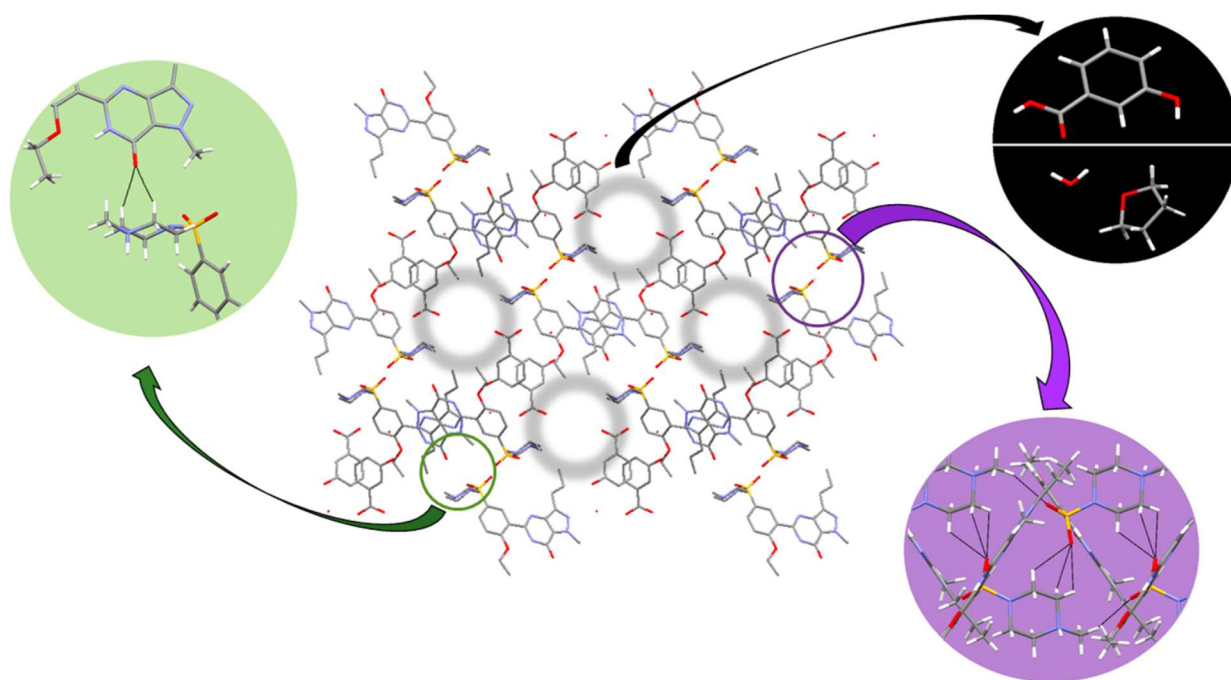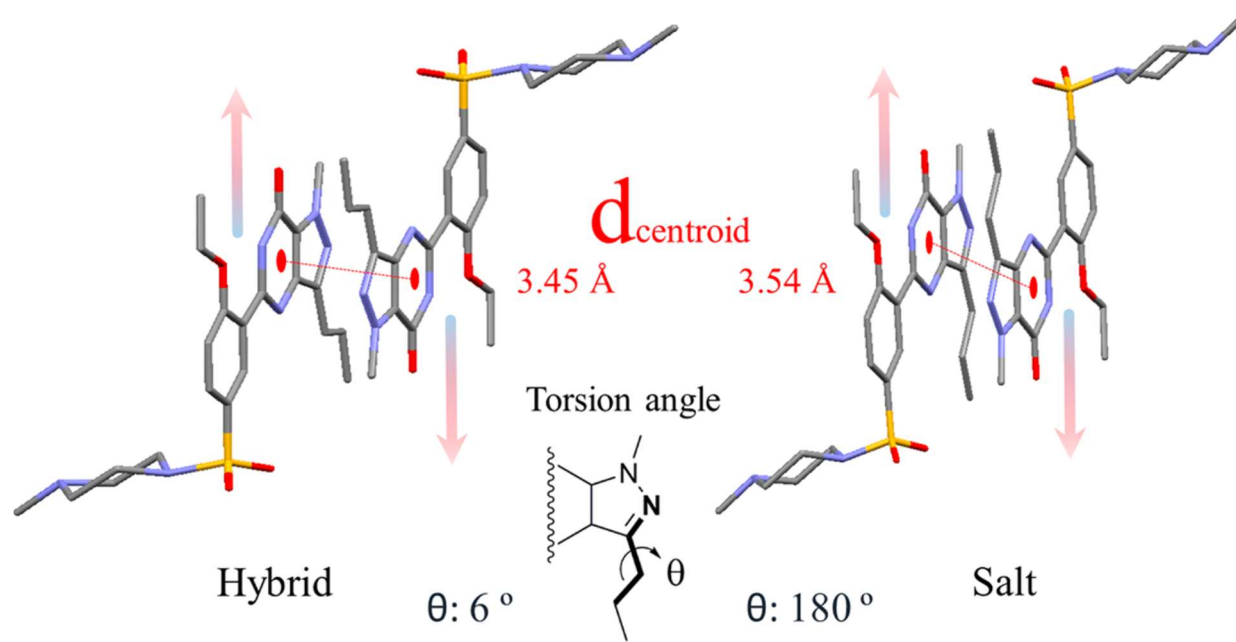
597 **FIGURE 9.**

598

599
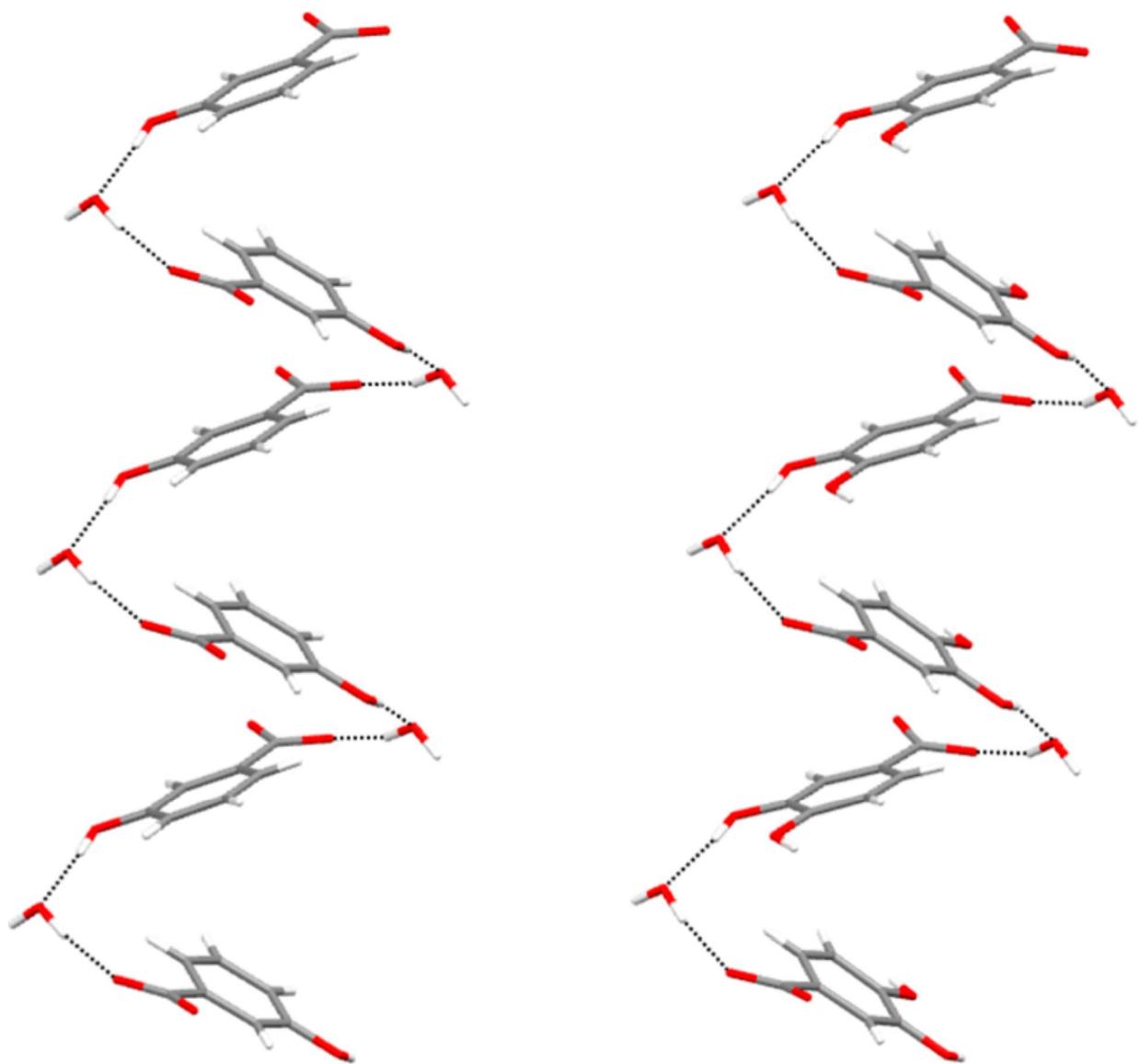
600

601

602 **FIGURE 10.**

603

604
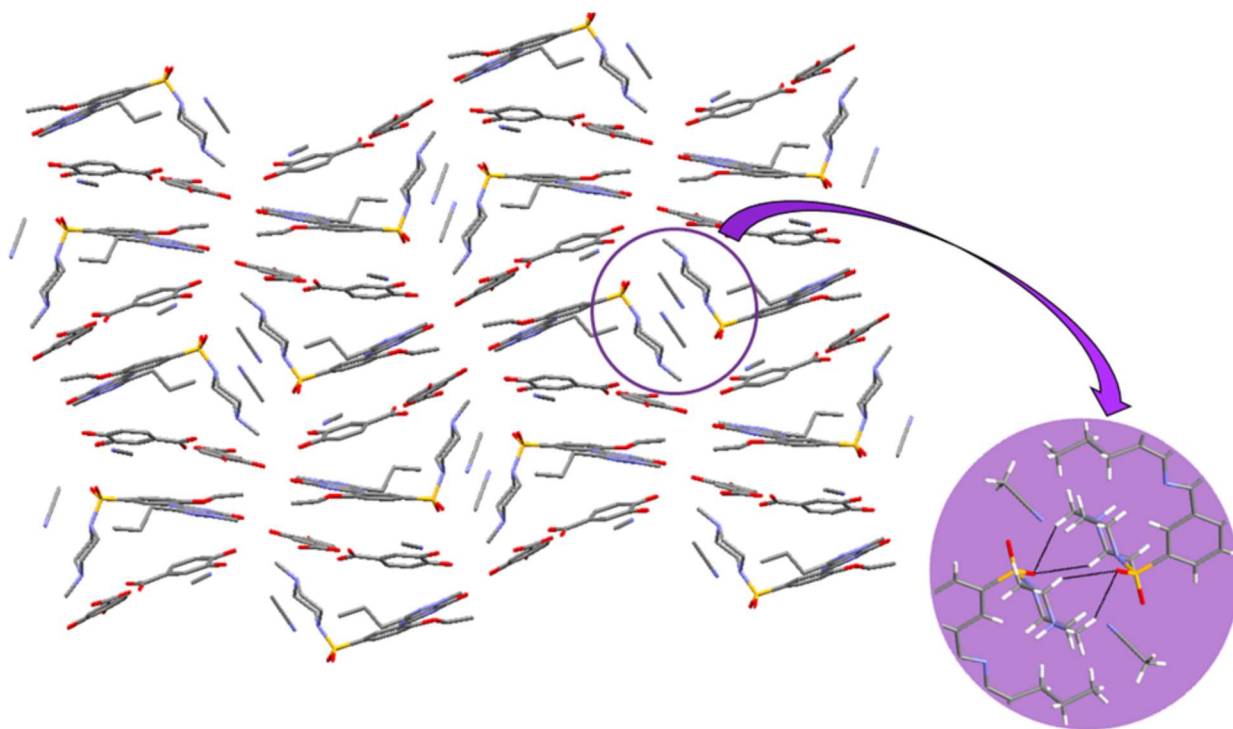
605

606

607

FIGURE 11.

608

609
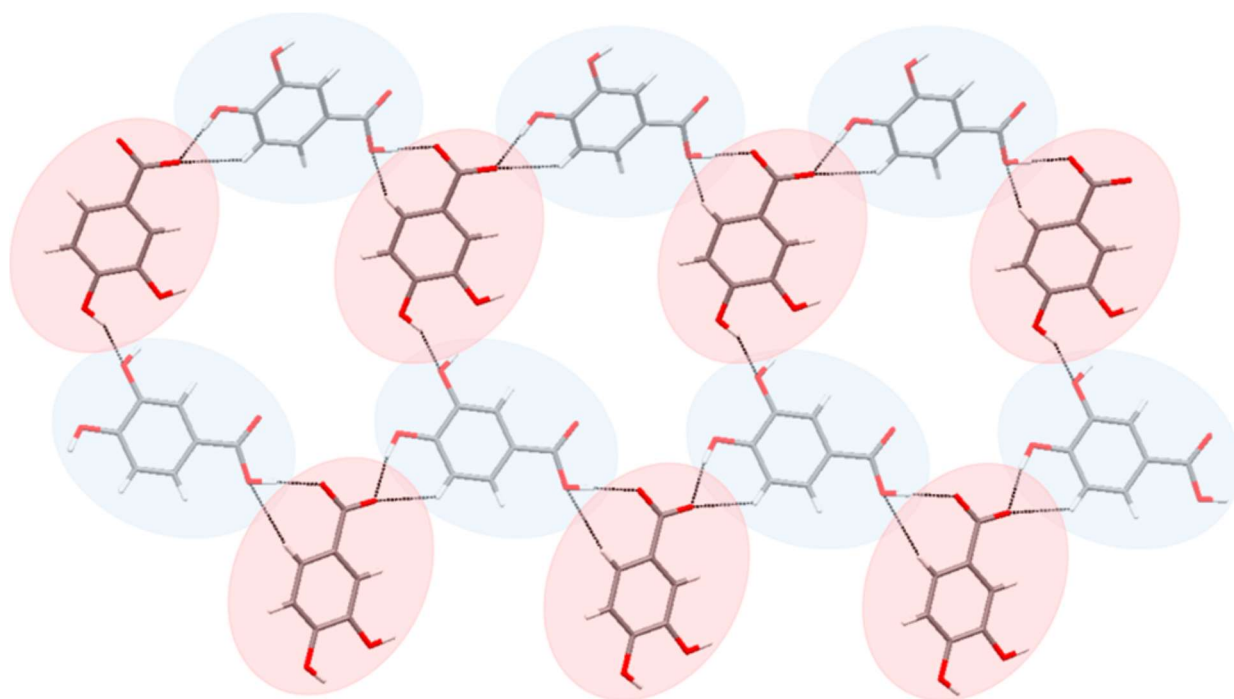
610

611

612

FIGURE 12.

613

614
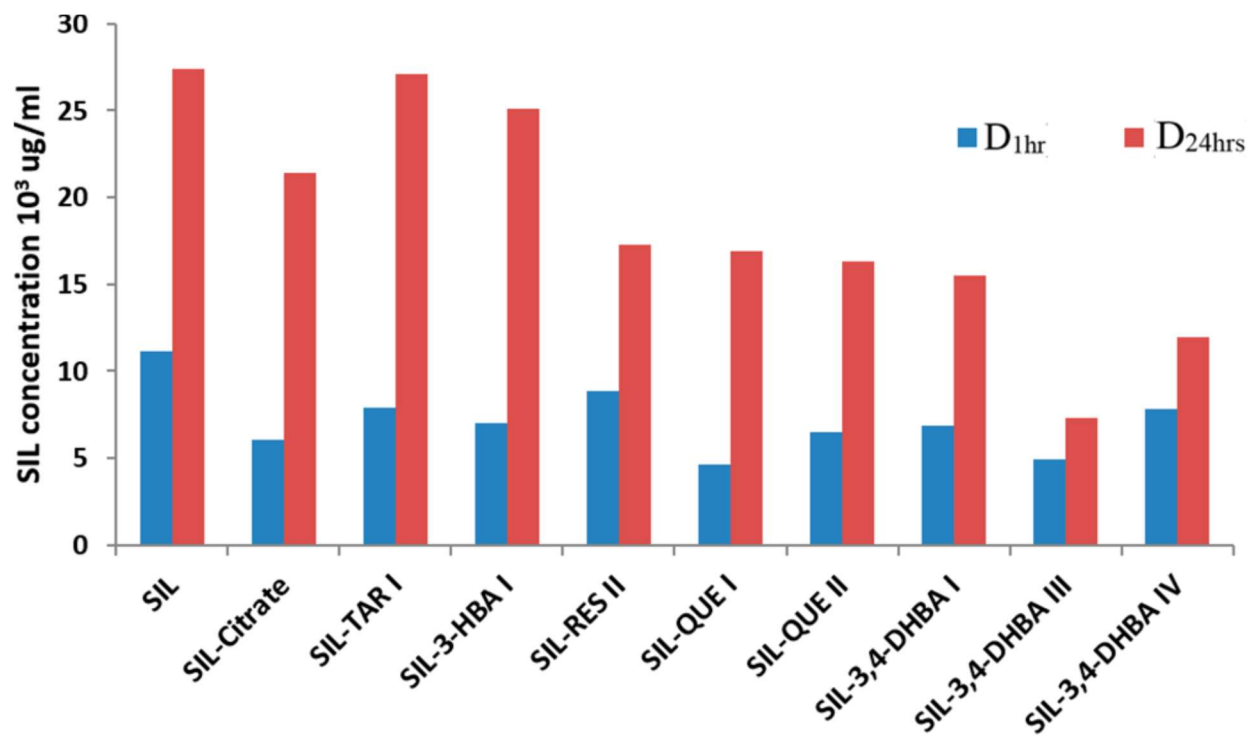
615

616

617

FIGURE 13.

618

619

620

621

622

FIGURE 14

624 .

625

626

627 **Table 1** Crystal Data for the Different Crystal Forms of Sildenafil
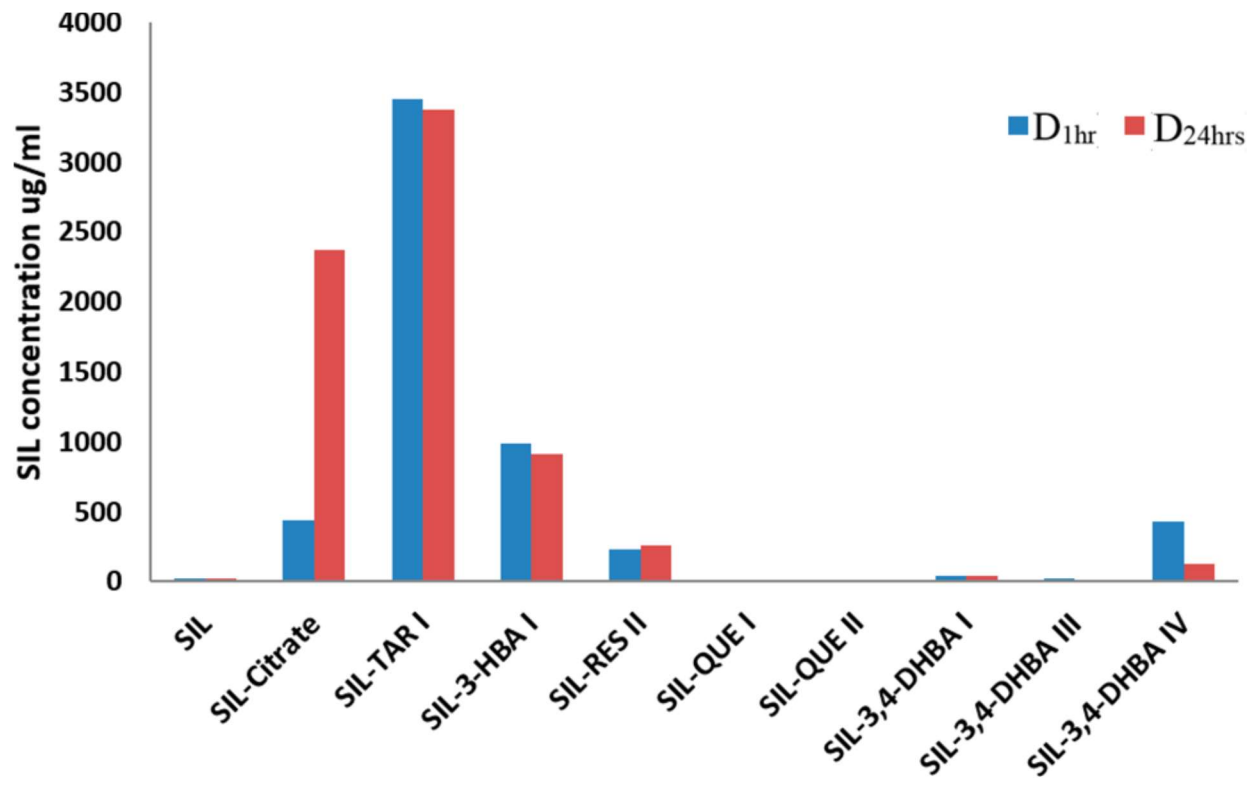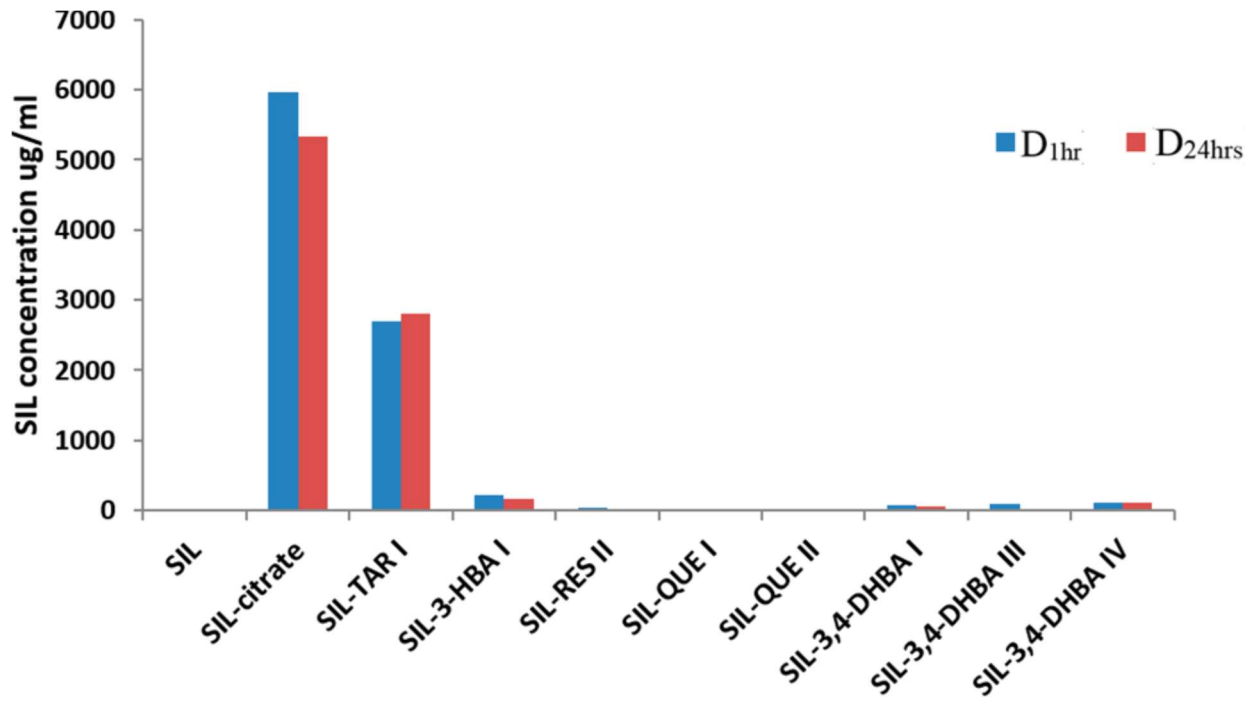
628

| structure	SIL-TAR IV	SIL-3,4-DHBA II	SIL-3,4-DHBA IV	SIL-3-HBA II	SIL-3-HBA IV
empirical formula	$C_{51}H_{74}N_{12}O_{15}S_{2}$	$C_{40}H_{48}N_{8}O_{12}S$	$C_{65}H_{82}N_{12}O_{11}S_{2}$	$C_{31}H_{41}N_{6}O_{9}S$	$C_{65}H_{82}N_{12}O_{19}S_{2}$
formula weight	1159.34	864.92	1447.54	675.77	1399.54
temperature (K)	293(2)	100(2)	100(2)	100(2)	100(2)
crystal system	triclinic	monoclinic	monoclinic	monoclinic	monoclinic
space group	P1̄	P21/n	P21/c	P21/n	P21/n
a, b, c (Å)	6.3796(8)	11.6418(8)	17.6070(17)	17.7205(18)	17.5329(10)
	13.4449(18)	15.3849(13)	8.6938(8)	8.2574(7)	8.6545(4)
	17.620(2)	24.7913(19)	24.942(2)	22.991(2)	22.9653(13)
α, β, γ (deg)	108.607(5)	90	90	90	90
	98.363(6)	102.749(3)	117.101(5)	102.748(3)	105.591(2)
	92.814(6)	90	90	90	90
volume (Å³)	1409.7(3)	4330.8(6)	3398.7(5)	3281.2(5)	3356.5(3)
Z, density (calc.) (Mg/m³)	1, 1.366	4, 1.327	2, 1.414	4, 1.368	2, 1.385
crystal size (mm³)	0.344 × 0.144 × 0.044	0.358 × 0.196 × 0.074	0.324 × 0.152 × 0.112	0.129 × 0.119 × 0.109	0.336 × 0.197 × 0.086
reflections collected/unique	53107/6455	66326/8875	69444/7838	18923/4567	33777/5726
	[R(int) = 0.1123]	[R(int) = 0.0949]	[R(int) = 0.0722]	[R(int) = 0.082]	[R(int) = 0.0482]
data/restraints/parameters	6455/8/396	8875/0/570	7838/2/460	4567/6/454	5726/0/502
goodness-of-fit on F^2	1.105	1.070	1.024	1.017	1.038
final R indices [$I > 2\sigma(I)$]	$R_1 = 0.0678$	$R_1 = 0.0537$	$R_1 = 0.0476$	$R_1 = 0.0504$	$R_1 = 0.0382$
	$wR_2 = 0.1740$	$wR_2 = 0.1151$	$wR_2 = 0.1084$	$wR_2 = 0.1168$	$wR_2 = 0.0886$
CCDC	1858573	1858576	1858577	1858574	1858575

629

630

Table 2. Comparative Cell Parameters Data[a] from SXRD and PXRD

crystal form		a (Å)	b (Å)	c (Å)	α (deg)	β (deg)	γ (deg)	V (Å³)	Z	R (%)	space group
SIL-QUE I	PXRD	42.39(2)	14.854(4)	15.059(6)	82.41(3)	138.08(2)	120.01(2)	4992(3)	5	11.1	P1̄
SIL-QUE II	PXRD	22.528(8)	13.536(4)	8.007(2)	57.95(2)	95.99(3)	95.96(2)	2054(1)	2	6.69	P1̄
SIL-3,4-DHBA I	PXRD	12.765(2)	13.463(1)	12.106(2)	112.03(1)	84.0929(9)	114.28(1)	1754.7(3)	2	8.41	P1̄
SIL-3,4-DHBA II	SXRD	11.6418(8)	15.3849(13)	24.7913(19)	90	102.749(3)	90	4330.8(6)	4	5.37	P21/n
SIL-3,4-DHBA III	PXRD	24.947(6)	15.718(3)	11.642(3)	90	103.96(2)	90	4430(2)	4	7.76	P21/n
SIL-3,4-DHBA IV	SXRD	17.6070(17)	8.6938(8)	24.942(2)	90	117.101(5)	90	3398.7(5)	2	4.76	P21/c
SIL-RES I	PXRD	11.266(2)	14.835(2)	14.178(2)	38.099(7)	94.79(1)	96.09(9)	1453.9(3)	2	12.0	P1̄
SIL-RES II	PXRD	14.2705(4)	26.083(2)	9.9925(5)	90	108.398(3)	90	3530.0(3)	4	6.20	P21/a
SIL-TAR I	PXRD	18.07(1)	13.609(6)	7.590(4)	85.98(3)	92.33(3)	110.09(4)	1749(1)	2	7.31	P1̄
SIL-TAR II	PXRD	33.57(9)	15.070(3)	11.547(3)	90	90	90	5445(2)	4	8.11	P21 21 21
SIL-TAR III	PXRD	18.313(4)	15.070(3)	6.3764(9)	63.85(1)	101.56(1)	112.86(2)	1454.5(5)	2	7.64	P1̄
SIL-TAR IV	SXRD	6.3796(8)	13.4449(18)	17.620(2)	108.607(5)	98.363(6)	92.814(6)	1409.7(3)	1	6.78	P1̄
SIL-CAF I	PXRD	25.845(7)	8.336(1)	20.32(6)	90	121.19(1)	90	3744(2)	2	5.76	P21/m
SIL-MG	PXRD	12.9869(8)	13.4289(8)	13.4551(8)	53.033(3)	118.580(4)	111.246(4)	1637.1(1)	2	5.04	P1̄
SIL-3-HBA II	SXRD	17.7205(18)	8.2574(7)	22.991(2)	90	102.7448(3)	90	3281.2(5)	4	5.04	P21/n
SIL-3-HBA IV	SXRD	17.5329(10)	8.6545(4)	22.9653(13)	90	105.591(2)	90	3356.5(3)	2	3.82	P21/n

[a] R-factor for SXRD and R_{wp} for PXRD.

631

632

633

634

635 **Table 3** Coformers Chosen in This Study Based on the Difference between the Interaction Site Pairing

636 Energies of Sildenafil and the Pure Components, ΔE

637

coformer	$\Delta E / kJ\,mol^{-1}$
quercetin	28.1
resveratrol	24.0
phloroglucinol	23.8
3,4-dihydroxybenzoic acid	21.7
resorcinol	19.3
tartaric acid	18.2
caffeic acid	17.8
myo-inositol	15.7
tert-butylhydroquinone	13.8
methyl gallate	13.5
3-hydroxybenzoic acid	13.1
4-hydroxybenzoic acid	12.9

638

639

640 **Table 4** Cocrystal Screening Coformers pKa's and Estimated Probability of Proton Transfe

641

coformer	reported pK_a	ΔpK_a	P (%)
quercetin	8.45[85]	−1.67	0
resveratrol	8.49[86]	−1.71	0
phloroglucinol	7.97[87]	−1.19	8
3,4-dihydroxybenzoic acid	4.40[87]	2.38	68
resorcinol	9.44[87]	−2.66	0
tartaric acid	3.03[87]	3.75	92
caffeic acid	4.47[86]	2.31	67
myo-inositol	12.29[86]	−5.51	0
t-butylhydroquinone	9.94[86]	−3.16	0
methyl gallate	8.11[85]	−1.33	5
3-hydroxybenzoic acid	4.08[88]	2.7	74
4-hydroxybenzoic acid	4.57[88]	2.21	66

642

643

644 **Table 5** Classification of Multicomponent Crystals with a Piperazine and a Carboxylic Group in the

645 CSD

class	no. of structures	%
salt	184	75
cocrystal	38	15
hybrid	25	10

646